Journal of Industrial and Engineering Chemistry 95 (2021) 148–155

Contents lists available at ScienceDirect

Journal of Industrial and Engineering Chemistry

journal homepage: www.elsevier.com/locate/jiec

Preparation of alginate hydrogel with human-derived adipose tissue to improve fat graft survival and adipogenesis

ByoungYong Yoo[a,1], Sujin Kim[i,1], Byung Ho Shin[f,1], Moon Hyun Lee[h], Young Bin Choy[e,f,g], Kangwon Lee[b,*], Chan Yeong Heo[c,d,e,**], Won-Gun Koh[a,***]

[a] Department of Chemical and Biomolecular Engineering, Yonsei University, Seoul, 03722, Republic of Korea
[b] Department of Applied Bioengineering, Graduate School of Convergence Science and Technology, Seoul National University, Seoul, 08826, Republic of Korea
[c] Department of Plastic and Reconstructive Surgery, Seoul National University, College of Medicine, Seoul 03080, Republic of Korea
[d] Department of Plastic and Reconstructive Surgery, Seoul National University Bundang Hospital, Seongnam 13620, Republic of Korea
[e] Interdisciplinary Program for Bioengineering, College of Engineering, Seoul National University, Seoul 08826, Republic of Korea
[f] Department of Biomedical Engineering, Seoul National University College of Medicine, Seoul 03080, Republic of Korea
[g] Institute of Medical & Biological Engineering, Medical Research Center, Seoul National University, Seoul 03080, Republic of Korea
[h] Nano Biomaterial Laboratory, Department of Polymer Science & Engineering, Sungkyunkwan University, Suwon, Republic of Korea
[i] Program in Nanoscience and Technology, Graduate School of Convergence Science and Technology, Seoul National University, Seoul, 08826, Republic of Korea

ARTICLE INFO

Article history:
Received 22 October 2020
Received in revised form 2 December 2020
Accepted 14 December 2020
Available online 24 December 2020

Keywords:
Human adipose tissue
Alginate-fat scaffold
Adipose tissue regeneration

ABSTRACT

Autologous fat and synthetic and natural polymers have been used as materials and scaffolds in adipose tissue (AD) regeneration, combining various polymers and biological components, including extracellular matrix molecules, decellularized matrix, and adipose-derived stem cells, which have been studied to improve the adipogenesis ability of scaffolds. This study used human AD as the scaffold material, with a great source of biomaterials closest to the human body. We report a simple and facile scaffold fabrication method using a natural polymer, alginate, and human AD and confirmed the adipogenesis ability *in vivo*. Scaffold fabrication was performed by simply mixing human AD with alginate and cross-linking in a non-cytotoxic way, using $CaCl_2$ solution. This method allows facile control of the shape and mechanical properties of the scaffold, which has great advantages in medical and aesthetic applications. *In vitro* experiments demonstrated the viability and secretion of adipokines in the scaffold. Four weeks of *in vivo* experiments showed that alginate protected human AD, which aided in AD survival, and that volume and shape were better preserved. Furthermore, we confirmed that our scaffold enhanced the adipose regeneration of the host animal and increased adipogenesis of the transplanted human AD by gene expression analysis.

Introduction

Loss of adipose tissue (AD) due to disease, trauma, and injury can seriously affect patients beyond physical trauma; damage/infection to appearances can adversely affect the emotional health of the patients [1,2]. In modern society, along with treatments for the loss of AD, fat transplantation and removal are frequently performed in the field of plastic surgery, where, with the development of medical technology, human life spans have extended and interest in the health and cosmetic aspects of life has increased [3]. Various materials have been studied for replacing or regenerating AD, including autologous fat, polymers that can fill up space where volume has been lost, and functional scaffolds that can induce adipogenesis [4]. Autologous fat has been widely used owing to its high biocompatibility and low immune response. However, studies on the reconstruction and regeneration of AD using autologous fat have revealed the following disadvantages [5]. Calcification occurs post-transplantation because of the lack of oxygen and nutrients due to low neovascularization [6], resulting in a low regeneration rate of AD. As a consequence, transplanted fats are rapidly degraded *in vivo*; the loss of up to 80%

* Corresponding author at: Department of Applied Bioengineering, Graduate School of Convergence Science and Technology, Seoul National University, Seoul, 08826, Republic of Korea.
** Corresponding author at: Department of Plastic and Reconstructive Surgery, Seoul National University Bundang Hospital, Seongnam, 13620, Republic of Korea.
*** Corresponding author at: Department of Chemical and Biomolecular Engineering, Yonsei University, Seoul, 03722, Republic of Korea.
E-mail addresses: Kangwonlee@snu.ac.kr (K. Lee), lionheo@snu.ac.kr (C.Y. Heo), wongun@yonsei.ac.kr (W.-G. Koh).
[1] These authors contributed equally to this work.

https://doi.org/10.1016/j.jiec.2020.12.015
1226-086X/

or more fats occurs within three months [7]. There is a further issue with the supply of materials: the quantity of fats that can be supplied by patients is limited to their surplus fats so transplantations that require a large quantity of fats are limited [8]. To address these issues, research has been conducted on developing polymers in the form of silicone or hydrogel, with physical properties similar to those of AD. These methods have the advantage of being semi-permanently implanted to replace the volume of the lost tissues. However, they lack biocompatibility compared to autologous fat transplantation and have side effects, such as rupture, capsular contracture, and excessive immune response [9,10]. To overcome the drawbacks of these conventional methods using autologous fats and polymers, functional scaffolds with the potential to improve adipogenesis in the transplanted area have been newly investigated [11]. In order to develop functional scaffolds that can promote adipose tissue regeneration, biodegradable/biocompatible polymers such as hyaluronic acid (HA), alginate and and poly(lactic-co-glycolic acid) (PLGA) have been studied. These polymers can be degraded after inducing AD regeneration and simultaneously cause less immune response than other polymers [12–16]. Furthermore, many studies have been conducted to improve the adipogenic ability of scaffolds by combining these materials with various biological factors that can improve adipogenic potentials, such as extracellular matrixes (ECMs), adipose-derived stem cells (ADSC), and growth factors [16–20]. For example, despite the increased AD regeneration, these attempts were still limited to utilizing only a part of natural AD regeneration, *e.g.*, certain proteins and cells.

In this study, we present a functional scaffold using AD itself as a scaffold material, rather than only ADSCs or growth factors, to induce the whole process of natural AD regeneration. To overcome the limitations of autologous fats that were previously stated, we chose alginate hydrogel as the other material to encapsulate the autologous fats to promote neovascularization and protect the autologous fat from rapid degradation *in vivo*. We also believe that alginate hydrogels can increase the volume capacity of the scaffold while maintaining the adipogenic ability of autologous fats. In addition, alginate is a material with various physical properties that are easily adjustable, depending on the calcium ion concentration, making it easy to fabricate scaffolds with physical properties that are similar to human AD. These advantages of alginate demonstrate the potential for a new material that can be used in AD regeneration. In this study, the alginate-fat scaffold was prepared by a facile method of mixing alginate in the sol state with fats from which blood cells were removed and cross-linked with calcium ions. AD and fat are commonly used as the same term but, in this study, AD refers to the whole tissue and fat to the purified AD, from which free oils, blood, and fibers are removed to avoid confusion. We successfully developed a functional scaffold that protects AD *in vivo* and has an AD regeneration effect. We fabricated an alginate-fat scaffold with properties similar to human AD, which is of aesthetic importance. We confirmed the increased survival rate of the alginate-fat scaffolds, neo-adipogenesis in the transplanted area, and reduced immune response, compared to the ADs and alginate gels up to 4 weeks post-transplantation *in vivo*.

Experimental

Materials

Alginate was obtained from NovaMatrix (Sandvika, Norway), and the solvent, Dulbecco's phosphate-buffered saline (DPBS), was supplied by Biowest (Nuaillé, France). Calcium chloride was purchased from Sigma Aldrich (St. Louis, MO, USA). AlamarBlue Cell Viability Reagent was supplied by Thermo Fisher Scientific (Waltham, MA, USA). The anti-Perilipin-1 antibody (ab61682) and donkey anti-goat IgG H&L (Alexa Fluor® 488) (ab150129) were purchased from Abcam (Cambridge, MA, USA).

Preparation of alginate-fat scaffold

Fig. 1 shows the procedures used to prepare each sample. Specifically, all harvested human ADs (IRB approval: B-1805-471-305) were washed three times in DPBS, with 1% penicillin/streptomycin. To prepare AD samples, human AD was cut into a cylinder with a weight of 200–220 mg. To prepare the alginate-fat scaffold (SC) samples, we chopped the AD and centrifuged at 1300 rpm for 3 min, with the same amount of DPBS with 1% penicillin/streptomycin [21]. We chopped adipose tissue in order to increase viability of cells in the core of the scaffold by mixing it homogeneously with alginate gel which facilitates nutrient and

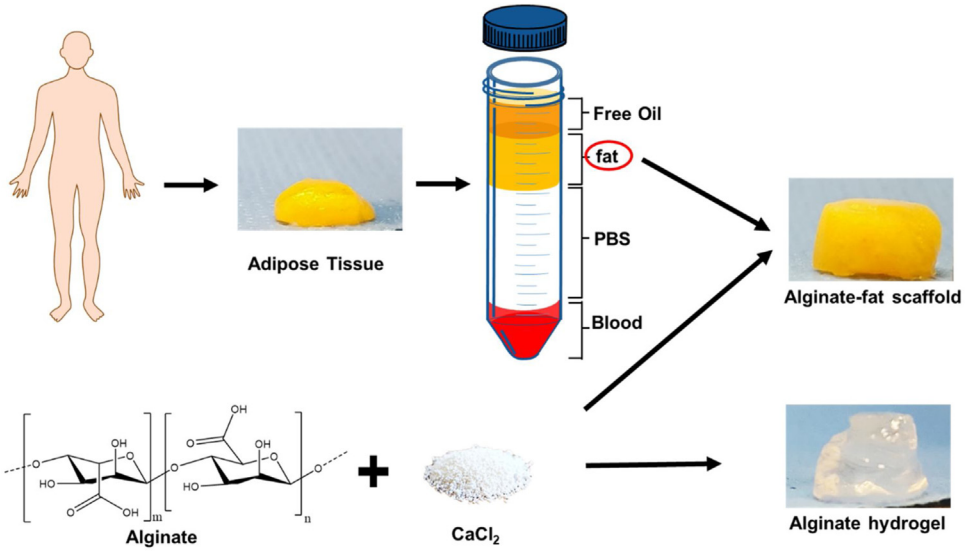

Fig. 1. Schematic illustration of the fabrication of alginate-fat scaffold.

oxygen transportation into the core of the scaffold. In addition, we used only purified fats after centrifugation that consist of ADSCs, adipocytes, and endothelial cells, necessary components for promoting adipose tissue regeneration [22]. At the same time, this purification step enabled fabrication of consistent scaffolds by helping chopped adipose tissue to mix with alginate precursor homogeneously. We discarded the top free oil layers and the aqueous layer and used the fat pellet for the following repeating procedure. After repeating the procedure three times, we added 250 μL of the fats, equal to 200–200 mg of AD, into the 48-well plate and then added 250 μL of alginate solution. SC could be fabricated in any form if there was a mold for it. We fabricated cylindrical scaffold because we could get well plates easily which have cylindrical wells that can be used as molds. We also judged that the cylindrical form was suitable for *in vivo* surgery. The alginate solution was prepared by stirring alginate powder (M. W > 200 kDa, Pronova) with 1% DPBS (w/v) and 1% penicillin/streptomycin (v/v). After mixing purified AD with an alginate solution, we added 68 mM $CaCl_2$ in DPBS solution and incubated at 37 °C for 3 h to fully cross-link the alginate. For the alginate (AL) sample, we did not add AD but used 500 μL of alginate solution, with the same concentration of $CaCl_2$ solution, and incubated at 37 °C for 3 h to prepare the alginate gel. After the cross-linking reaction, the remaining $CaCl_2$ was removed by washing several times with DPBS. Three kinds of samples were uniformly fabricated in a cylindrical form which have the same distance between core of samples and outside of samples in order to minimize variances on viability and adipose tissue regeneration caused by the shape of samples such as transportation of nutrients and oxygen.

Mechanical properties of adipose-alginate scaffold

The dynamic shear modulus at 10% deformation was used to measure the viscoelastic properties of alginate-fat scaffolds, depending on different concentrations of alginate at a ratio of 1:1 to fat and different ratios of fat:1 w/v% alginate. AD and AL were also measured as references. AD was used as a reference with optimal viscoelastic properties, such as human AD, as it is unprocessed after being collected from a patient. Rheological measurements under vibration-shear strain were performed on an MCR 102 (Anton-Paar of Australian Graz material) using a 20 mm Peltier plate steel with a plate-large-plate distance of 10 mm. The storage modulus was recorded in constant deformation mode, with a deformation of 10% maintained over a frequency range of 0.1–300 Hz (rad/s), at 25 °C [12].

Alamar blue assay to measure in vitro *viability of AD and SC*

The AD and SC samples were incubated with 1 mL DMEM 10% FBS and penicillin (100 U/mL) at 37 °C in a 24-well plate. Alginate hydrogels (250 mL) were cultured together to measure the background signal of alginate hydrogels in SC. Alamar blue assay was performed on day 0, 1, 4, and 7 according to previously used methods [23]. The measurement on day 0 proceeded immediately after the samples were prepared to measure the initial bioactivity. At each time point, the samples were washed three times with DPBS and placed into a new 24 well plate. A culture medium (1 mL) with 10% alamar blue reagent (w/v) was added and cultured for 6 h. The background signal of AD was measured from 1 mL of culture medium with 10% Alamar blue reagent (w/v). Finally, fluorescence intensity (Ex570 nm, Em 610 nm) of 100 mL culture medium from each sample was measured using a microplate reader (Spectra MAX GEMINI EM, Molecular Devices, San Jose, CA, USA). The blank value was subtracted from the AD value to remove the background signal and the value of 250 mL alginate hydrogel was subtracted from the value of SC to remove the background signals of SC originating from the alginate portion. Since the initial number of cells present in AD and SC was different, the values at days 1, 3, and 7 were divided by the value at day 0 to confirm the relative biocompatibility of the initial value.

Antibody array to measure adipokines

Various growth factors related to AD regeneration are released along with adipogenesis during AD culturing [24,25]. We measured and profiled the growth factors released during culturing of the sample. The AD, SC, and AL samples were cultured in 1 mL DMEM and supplemented with 10% FBS and 1% penicillin (100 U/mL) at 37 °C and 5% CO_2 in a 24-well plate. We included 1 mL of culture medium for measuring background signals and AL was also included as a negative control for the alginate part of the SC. After culturing for seven days without changing the medium, Proteome Profiler Human Adipokine Array Kit (R&D Systems, Minneapolis, MN, USA) was performed based on the protocol of the product using AD, SC, AL, and blank culture supernatants. The density of the dots was measured using Image J software (ver. 1.47, National Institutes of Health, MD, USA, MD), and final values were obtained by dividing the adipokine dot density by the reference dot density.

In vivo *experiments*

The animal experiment protocol was approved by the Animal Care and Use Committee (IACUC) of Seoul National University Bundang Hospital (BA1805-247/042-01). Six-week-old SKH-1 hairless mice were grown under specific-pathogen-free (SPF) conditions, allowed free access to food and water, and maintained in a 12/12-h light/dark cycle. In this study, animals were randomly divided into three separate groups, transplanted into AD, SC, and AL. Five mice, totaling ten mice for each sample type, were assigned to two different biopsy times, 2 and 4 weeks post-transplant. After the mouse was anesthetized with isoflurane, The surgical site (center of the dorsal region) was sterilized with betadine. A subcutaneous pocket was made using with a surgical scissor and each sample was inserted into the pocket. After suturing the incision with a nylon surgical suture (3/0 nylon B430,

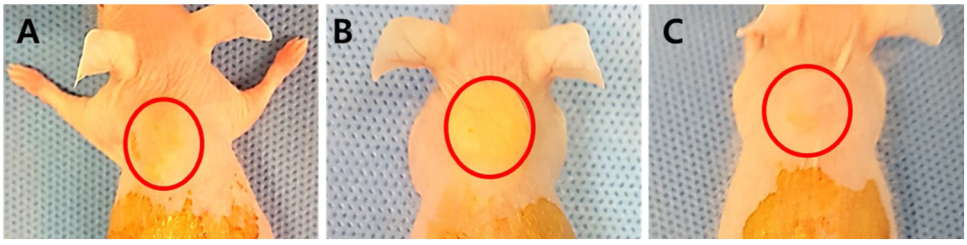

Fig. 2. Photographs of transplanted area. The samples are AD, alginate-fat scaffold, and alginate hydrogel, from the left.

WooRiMedical, Korea), it was presented with an intraperitoneal gentamicin injection of 20 mg/kg. Fig. 2 shows the mice after transplanting each sample. Each sample was biopsied at scheduled intervals and fixed with 4% paraformaldehyde.

In vivo *evaluation*

Hematoxylin and eosin (H&E) staining

Each tissue was stained with hematoxylin-eosin for inflammation analysis. For deparaffinization, the tissue slides were incubated at 60 °C for 1 h to melt the paraffin and soaked in xylene three times for 5 min each. Deparaffinized slides were sequentially immersed in 100%, 95%, 90%, 80%, 70%, and 50% alcohol for 5 min to produce stains. After hydrating the slides, they were stained with a hematoxylin-eosin working solution for H&E staining.

Immunofluorescence staining

After deparaffinization and rehydration, perilipin was immunostained for analysis of the necrotic area. For IF staining, the slides were first incubated with an antigen-retrieval solution and microwaved for 15 min. After cooling at 25 °C the slides were washed three times for five min at a pH of 7.4 PBS. The slides were then treated with goat serum solution for 1 h to block nonspecific antigen binding. The slides were then incubated overnight with the primary antibody diluted from the dark chamber. The anti-perilipin-1 antibody was used at a 1:200 dilution. Subsequently, the slides were diluted with donkey anti-goat IgG H&L (Alexa Fluor® 488) at 25 °C for 1 h at 1:2000 and then cultured. The slides were then thoroughly washed and stained with DAPI to stain the cell nuclei.

Liquid replacement method

To measure the volume of AD, SC, and AL implanted in the mice, the biopsy was performed at 2 and 4 weeks and the tissue was cleanly removed from the implanted site. The sample volume was measured by subtracting the initial volume of liquid from the volume after the sample was completely submerged. Chloroform was used to measure the liquid.

Reverse transcription polymerase chain reaction (RT-PCR)

The biopsy mouse tissue samples were frozen and stored in liquid nitrogen immediately after biopsy and the total mRNA was isolated from the mouse tissue samples using Trizol reagent (Invitrogen, USA). Complementary DNA (cDNA) was synthesized using RevertAid Reverse Transcriptase (RevertAid First Strand cDNA Synthesis Kit, Thermo Scientific, Waltham, MA, USA). PCR analysis was conducted using a cDNA template with primers specific for human adipocyte fatty acid-binding protein (aP2), adiponectin, and β-actin. Expression of the housekeeping gene β-actin was used as an internal control. The PCR products were electrophoretically separated on a 2% agarose gel and stained with ethidium bromide. Detailed information on the primers is provided in Table 1.

Statistical analysis

All values are shown as All values are shown as the mean ± SD. All data were analyzed using GraphPad Prism 7 (GraphPad Software Inc., La Jolla, CA, USA). Significance was calculated using a one-way analysis of variance with the Tukey post hoc test and $p \leq 0.05$ was considered significant. *In vitro* and *in vivo* data were obtained from five samples (n = 5). Error bars represent the standard deviation.

Results

Shape of the prepared AD, SC, and AL

The shapes of the AD, SC, and AL samples are shown in Fig. 1. AD samples were prepared in the range of 200–220 mg by weight but the shape was not uniform in each sample. SC samples had a uniform cylindrical shape with perfect reproducibility.

Mechanical properties of AD, SC, and AL

A rheometer measured the mechanical properties of AD, AL, and SC (Fig. 3). The most important element of a material that maintains its structure is its mechanical properties. We aimed to fabricate a sample with the most similar mechanical properties to human AD. For this purpose, we measured the storage modulus of SCs with various alginate concentrations at a volume ratio of 5:5 to fat and confirmed that SC had the most similar storage modulus (2000–3000 Pa) to AD, which is the human AD when the concentration of alginate solution was 1% (Fig. 3A) [12]. We also measured the storage modulus of the SCs, depending on the ratio of fat to 1% alginate (Fig. 3B). We confirmed that a volume ratio of 5:5 had the most similar storage modulus to AD. The adipose tissue used in the measurements in Fig. 3A and B were obtained from different patients. Due to age and gender differences, there was a

Table 1
List of primers used for the RT-PCR.

Gene bank accession no.	Gene	Forward and reverse primer sequences	Annealing temperature (°C)	Product size (bp)	Origin
NM001442	aP2	5′-TGC AGC TTC CTT CTC ACC TTG A-3′ 5′-TCC TGG CCC AGT ATG AAG GAA ATC-3′	55	256	Human
NM024406		5′-GAA TTC GAT GAA ATC ACC GCA-3′ 5′-CTC TTT ATT GTG GTC GAC TTT CCA-3′	55	94	Mouse
NM004797	Adiponectin	5′-TGG TGA GAA GGG TGA GAA-3′ 5′-AGA TCT TGG TAA AGC GAA TG-3′	50	221	Human
NM009605		5′-CAA GGG AAC TTG TGC AGG-3′ 5′-CGT GAT GTG GTA AGA GAA GTA G-3′	50	400	Mouse
NM000230	Leptin	5′-TCT TGT GGC TTT GGC CCT ATC T-3′ 5′-CCA GTG TCT GGT CCA TCT TGG ATA-3′	55	181	Human
NM008493		5′-TGC TGC AGA TAG CCA ATG AC-3′ 5′-GAG TAG AGT GAG GCT TCC AGG A-3′	55	142	Mouse
NM001101	β-actin	5′-TGACGGGGTCACCCACACTGTGCCCATCTA-3′ 5′-CTAGAAGCATTTGCGGTGGACGATGGAGGG-3′	60	663	Human
NM007393		5′-TGG AAT CCT GTG GCA TCC ATG AAA C-3′ 5′-TAA AAC GCA GCT CAG TAA CAG TCC G-3′	60	349	Mouse

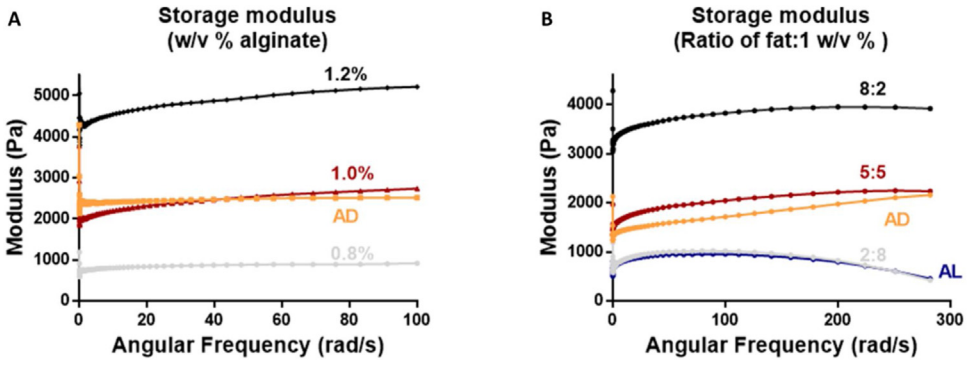

Fig. 3. Storage modulus of alginate-fat scaffold depending on (A) alginate concentration and (B) ratio of fat:1 w/v % alginate.

difference in the storage modulus of samples made of AD in both figures. However, since the two measurements are independent of each other, the sample with the storage modulus most similar to AD could be identified by comparing AD and other samples in each measurement. The results show that the rheological properties of the SC depended on the concentration of alginate, as well as the ratio of fat to alginate, and it is controllable.

In vitro *evaluation*

In vitro *viability of AD and SC*

The *in vitro* cell viability of AD and SC was determined using the alamar blue assay (Fig. 4A). The viability increased in both AD and SC on day 1, as compared with day 0, and the values increased steadily at day 4 and day 7. This result indicates that cells in AD and SC were viable *in vitro*. In addition, AD showed approximately two times higher values than SC, at all time points.

In vitro *secretion of adipokines of AD and SC*

The Proteome Profiler Human Adipokine Array Kit was used to profile the expression of 58 human adipokines in AD and SC (Fig. 4B). AL and blank (media) were also measured but adipokines other than the reference dot was not measured and data are not included in Fig. 4B. Among the 58 human adipokines, there were statistically significant differences in 27 proteins between AD and SC ($p \leq 0.05$). Among them, insulin-like growth factor-binding protein 6 (IGFBP-6) (blue box) and interleukin-6 (IL-6) (red box) showed the most significant differences ($p \leq 0.001$).

In vivo *evaluation*

Inflammation analysis

We performed *in vivo* tests using hairless mice and determined the degree of inflammation in each sample (Fig. 5). When the inflammatory response to AD was analyzed, it was confirmed that the inflammatory cells penetrated the AD and the foreign body reaction caused severe inflammation. This phenomenon slightly decreased at 4 weeks, rather than at 2 weeks, but the inflammatory response continued. In contrast, when AL was inserted, the inflammatory response of the host animal was mild. Similarly, SC showed a mild degree of inflammation and no statistical difference compared to AL.

Transplanted sample survival and volume change

In addition, when tracking the volume change of each transplanted sample, we confirmed that the volume of all the groups decreased compared to the initial volume (Fig. 6A). AD and AL showed a similar decrease in volume, but the SC was

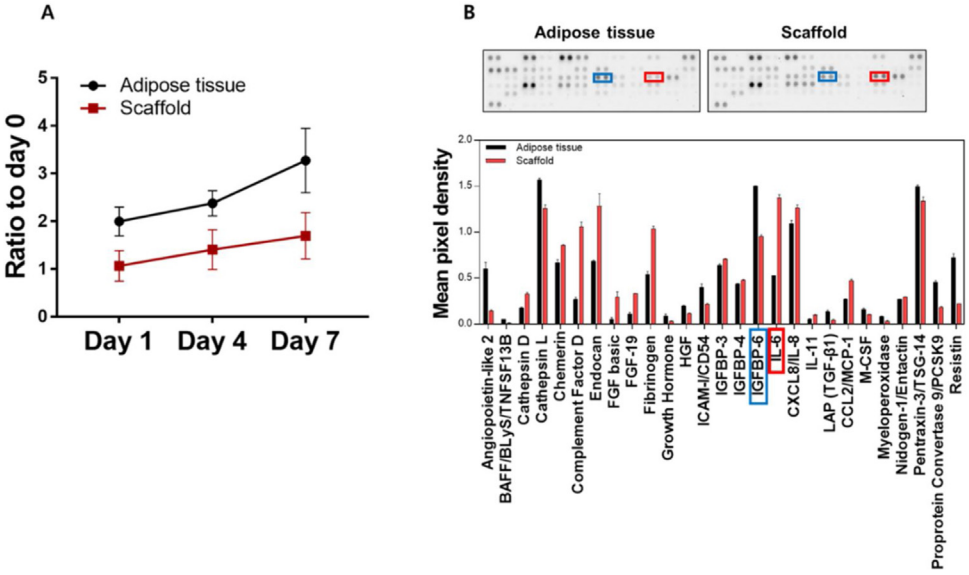

Fig. 4. (A) Cytocompatibility of AD and scaffold analyzed using alamar blue assay. (B) Profiling adipokines secreted by AD and scaffold using Proteome Profiler Human Adipokine Array Kit. Among 58 adipokines, 27 adipokines which showed significant difference ($P < 0.05$) between AD and scaffold were plotted on the histogram. The red and blue boxes indicate IL-6 and IGFBP-6 respectively, which showed the most significant difference.

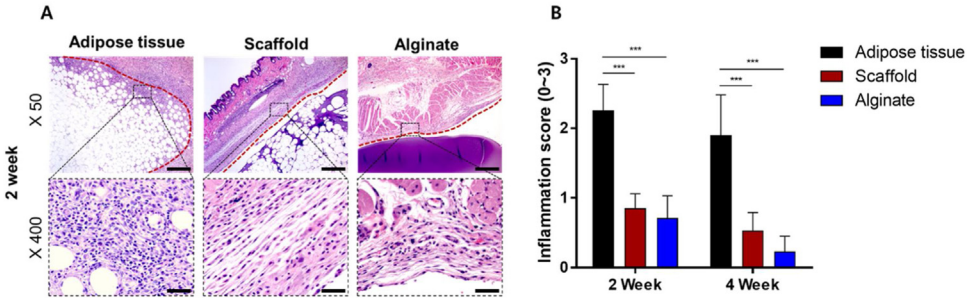

Fig. 5. Inflammation analysis of the samples. Representative histological images obtained at 2 weeks. The red dashed line indicates the position of the sample. The scale bars are 400 μm for ×50 and 50 μm for ×400. The histogram shows quantitative results at 2 and 4 weeks. Scores were calculated *via* a semiquantitative method. The asterisk (***) represents a statistically significant difference ($P < 0.001$).

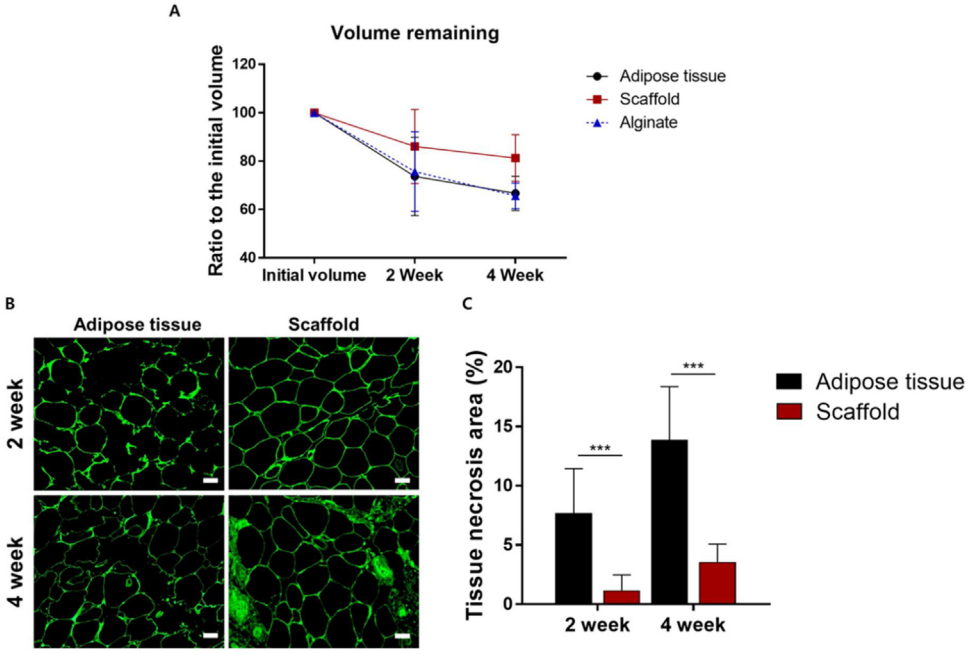

Fig. 6. (A) Graph of volume change in samples after implantation and (B) necrosis analysis. Representative histological images obtained at 2 and 4 weeks after sample implantation. The scale bars are 50 μm. The histogram shows the quantification of necrotic areas in anti-perilipin-1 staining. The asterisk (***) represents a statistically significant difference compared with the scaffold group with the AD group ($P < 0.001$).

confirmed to show high volume retention. When the survival of adipocytes in AD and SC were analyzed through immunofluorescence staining of Perilipin-1, as shown in Fig. 6B, the AD was already necrotic from 2 weeks and approximately 7.7% of the tissue had already collapsed. Conversely, the SC showed an intact adipocyte membrane with a low degree of necrosis. At 4 weeks, the AD necrosis progressed further, with 13.9% necrosis, and the SC was observed to have a slight progression of necrosis in the middle ($P < 0.001$). Checking for neovascularization in and out of a sample is a widely used method of confirming mass transfer into and out of a sample. However, in our study, it is possible to exchange materials into the sample without neovascularization through the alginate gel's porous structure. Therefore, rather than observing neovascularization, we observed the adipocyte membrane to confirm necrosis inside the sample.

In vivo *AD regeneration*

RT-PCR was performed on aP2, adiponectin, and leptin in biopsy samples at 4 weeks to compare adipogenic gene expression levels (Fig. 7). When the human genes were analyzed, it was confirmed that no bands were expressed except for aP2 in AD; however, aP2, adiponectin, and leptin were all found in SC. In

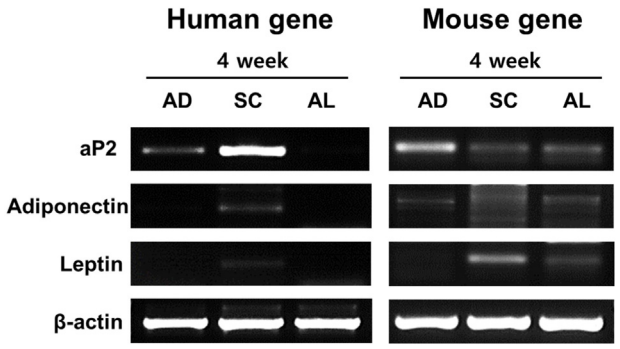

Fig. 7. RT-PCR analysis of gene expression for adipogenic differentiation in the implanted samples. Each gene (adipocyte fatty acid-binding protein (aP2), adiponectin, leptin, and β-actin) was analyzed with primers designed from human and mouse origins.

particular, aP2 was confirmed to be strongly expressed in SC. In mouse genes, bands of aP2 and adiponectin were observed in AD and aP2 was expressed more strongly than the scaffold. However, it was confirmed that the expression of aP2, adiponectin, and

leptin was evenly expressed in SCs. In AL, gene expression was similar to SC.

Discussion

Many attempts have been made to overcome the limitations of polymers in AD regeneration. The autograft procedure has been conducted most frequently for AD reconstruction; however, it still has drawbacks. We fabricated an alginate-fat scaffold and showed successful survival and enhanced adipogenesis. These results indicate that the alginate-fat scaffold can overcome the limitations of polymers and drawbacks of autograft and can be used for allograft or enhanced autograft operations.

When we prepared samples, AD samples were cut into cylindrical shapes with the same weight and shape as SC and AL. However, there was a disadvantage in that the quality of samples changed depending on the state of the AD of the patient, which was not easily maintained as uniformly cylindrical. These disadvantages are applied to patients who have undergone autologous fat transplantation, which results in the collapse of the postoperative shape and an inconsistent operation as the state of the AD is determined depending on the condition of the patient at the time of surgery. In the case of AL samples, fabricating a perfect cylinder shape was impossible because the surface directly contacting $CaCl_2$ was first cross-linked and the cross-linked alginate hydrogel blocked the further permeation of $CaCl_2$ solution into the center. Therefore, the resultant AL samples have inhomogeneous mechanical properties with a strong outer region and a weak inner region, making it difficult to prepare the sample with a perfect cylindrical shape. These results were compared with SC samples, which retained the perfect cylindrical shape with perfect reproducibility. The AD at the core of the alginate gel, especially the ECM inside the AD, causes morphological stability of the SC sample [26]. When we mixed alginate gel precursor with chopped adipose tissue, they were mixed thoroughly forming homogeneous mixture. The chopped adipose tissue was distributed homogeneously and maintained homogeneity within alginate scaffolds after crosslinking by $CaCl_2$. Reproducibility to fabricate samples with a uniform shape is important in AD engineering because they function as a filling material.

We also controlled the mechanical properties of alginate-fat scaffolds by varying the alginate concentration and fat:alginate ratio. The storage modulus of alginate-fat scaffolds increased with increasing alginate concentration and higher fat:alginate ratio (Fig. 3A, B). We reason that as the fat ratio became high, the ECM contents also increased, increasing the stability of the alginate structure and thus increasing the modulus that gives resistance to deformation; this also explains why adding fat into alginate was able to bring structural stability of the SC. Based on these results, it was confirmed that SC samples using a concentration of 1.0 w/v % alginate at a ratio of 5:5 to AD have the most similar rheological properties to human AD. We used SC samples fabricated under the condition that 1.0 w/v % alginate at a ratio of 5:5 for *in vitro* and *in vivo* experiments. Pore structure of SC, which is a homogeneous mixture with alginate gel, plays a critical role in increasing SC's survival rate *in vivo*. According to previous study, hydrogel made with 1 w/v% alginate possessed pores larger than 200 μm [27]. This makes it possible to exchange nutrients and through alginate gel in SC, and it was assumed that it would increase the survival of internal adipocytes and ADSCs, and this was confirmed in Fig. 6B and C [28].

We investigated the *in vitro* viability of AD and SC and the secretion of adipokines through biological activities. SC showed relatively low viability from day 1 to day 7, compared with AD, because centrifugation during the purification affected viability of cells in SC (Fig. 4A). It was reported that centrifugation of adipose tissue can affect viability of cells in the purified adipose tissue even in low speed (1200 rpm) that we used for purification [29]. However, both AD and SC showed a steady increase in measured values from day 1 to day 7, indicating that the process of purifying AD to make SC did not have critically adverse effects on cell viability. We next profiled the expression of 58 human adipokines in AD and SC using supernatant media cultured for 7 days. Both AD and SC showed similar dot densities for most proteins but showed the largest statistical difference in IGFBP-6 (blue box) and IL-6 (red box) (Fig. 4B). IGFBPs modulate insulin growth factor (IGF)-induced cell proliferation by promoting or inhibiting it [30,31]. Among them, IGFBP-6 binds to IGF and inhibits IGF action, which promotes the proliferation of cells in AD [32]. As more IGFBP-6 was detected in AD than in SC, the proliferation of cells in AD is expected to be suppressed by IGFBP-6 compared to SC. However, the *in vitro* culture showed that AD proliferated better than SC (Fig. 4A). We believe that this is because the concentration of IGF was not affected by IGFBP-6 *in vitro* culture. It can affect *in vivo* transplantation, which has IGF sources other than AD. The other adipokine showing the most significant difference between AD and SC is IL-6, which is known to modulate the acute immune response to injury or infection [33,34]. Bastard et al. confirmed a significant correlation between the IL-6 levels in AD and obesity; a higher IL-6 production from AD is related to an increase in total fat mass [35]. As more IL-6 was found in SC than in AD, IL-6 in SC would have had a greater impact on AD production than in AD. Although the roles of IGFBP-6, IL-6, and other adipokines in adipogenesis have not been identified, we confirmed that altering the environment of AD through the scaffolding process created significant differences in adipokine secretion. We expect these differences to further serve as a factor affecting AD's survival and adipogenesis *in vivo*. We exposed adipocytes, and ADSCs in purified AD through scaffolding to an environment of a homogenous mixture with alginate gel, so that facilitated transportation of nutrients through alginate gel and interaction with alginate gel induced adipokine secretion. We confirmed that. The same phenomenon explains this change in ADSC's paracrine ability due to the cell-material interaction as the study of Liu et al. confirmed different amounts of vascular endothelial growth factor secretion in scaffolds made of different materials [36].

In general, when xenografts or allografts are transplanted, rather than autografts, they are strongly attacked by the immune cells of the host [37,38]. A common transplanted tissue scenario is that the transplanted tissue breaks down and decreases in volume because of the strong immune response [39]. In this study, we confirmed that the immune response was reduced when the human AD was transplanted in the form of a scaffold using alginate (Fig. 5). Alginate reduced the surface area of human AD directly exposed to the host body. It acts as an immunogenic barrier in that it protects transplanted human AD from the infiltration of host immune cells and further immune response.

After four weeks of tracking the transplanted sample volume, it was confirmed that the SC was able to maintain the initial volume more successfully than the AD and AL (Fig. 6A). Inflammatory reactions and internal tissue necrosis are factors that reduce the AD volume. Eto et al. defined three zones of adipose autografting depending on the viability of the graft after transplantation, as follows [39,40]. Adipocytes can survive only in the surviving zone, which is less than 300 μm from the surface. Necrosis occurs in the necrotic zone, which is the most central zone due to deficiency of oxygen and nutrients. In the regenerating zone, between the surviving and necrotic zones, adipocytes die but stem cells can survive and dead adipocytes are replaced with host adipocytes. In our study, the surviving zone can be defined as the AD in Fig. 5, *i.e.*, the area less than 300 μm from the red dashed line. Adipocytes in this surviving zone were exposed to an inflammatory response because of the heterogeneous immune response. Inflammatory cells infiltrated AD and decreased the volume of AD (Fig. 6A).

Necrosis in the central zone also contributed to a decrease in the volume of AD (Fig. 6B). In the case of AL, three factors are considered to contribute to volume reduction. First, the immune response reduced the volume of AL degrading alginate. Second, the physical compression exerted by the skin tension was applied to AL, contributing to the volume reduction of AL. At the time of biopsy, the AL samples were in the form of a compressed ball, unlike the initial form, as shown in Fig. 1. Lastly, the decrease in water content caused by the difference between the water content of the initial alginate hydrogel and that of the mouse body contributed to the volume reduction. However, in the case of SC, alginate protected the transplanted AD from the infiltration of inflammatory cells (Fig. 5). Less necrosis occurred (Fig. 6B) because the porous structure of the alginate hydrogel facilitated the exchange of oxygen and nutrients into the central area of the SC. In addition, we reasoned that the decrease in volume loss of SC compared with AL is derived from changes in structure and composition that occurred after alginate was mixed with adipose tissue. In SC, structural stability of alginate increased after mixed with adipose tissue and this change reduced compression of SC caused by tension of mouse skin. And less amount of alginate in SC than in AL resulted in less volume reduction caused by water loss of alginate gel.

aP2, adiponectin, and leptin play important roles in lipid storage and glucose metabolism as representative adipogenesis markers [41,42]. Comparing AD with SC, the adipogenesis-related mRNAs of transplanted human AD were higher in all three genes in the SC group, indicating that alginate sustained the adipogenesis ability of human AD longer, until week 4. We speculated that mouse genes are expressed mainly due to host immune response. aP2 is known to relate not only with adipogenesis by adipocytes, but also with inflammatory activity by macrophages [43]. And leptin is known as a proinflammatory cytokine that has an important role in T cell activities [44]. We speculate that strong expression of mouse aP2 in AD was caused by intense inflammation in AD observed in Fig. 5 and leptin was stimulated by immune response to alginate because we could find leptin expression in SC and AL, not in AD.

Conclusion

This study fabricated an alginate-fat scaffold for AD regeneration using alginate and purified AD. The scaffold formed more easily into the desired shape and maintained the shape better for 4 weeks of *in vivo* experiments, compared to AD or alginate alone. These results show great advantages in terms of volume recovery and scaffold maintenance. Furthermore, analysis of the adipogenesis-related human genes confirmed that alginate protected the AD in the scaffold and helped deliver oxygen and nutrients, thereby improving the adipogenesis ability of the transplanted human AD. In addition, adipogenesis-related mouse genes were investigated and confirmed that the AD regeneration of the host was also enhanced in the scaffold. Overall, with this facile scaffolding of human AD, we expect that the drawbacks of autografts and limitations of polymers that have been researched for adipose regeneration will be overcome and allografts can be used for AD regeneration, even though this scaffolding method can still be applied to autografts.

Declaration of Competing Interest

The authors report no declarations of interest.

Acknowledgments

This research was supported by the National Research Foundation of Korea (NRF) funded by the Ministry of Science, ICT, and Future Planning and the Korea government (MSIT) (2020M3A914039045, 2016M3A9B4919711 and 2018M3A9E9071162).

References

[1] A. Alhadlaq, M. Tang, J.J. Mao, Tissue Eng. 11 (2005) 556.
[2] A. Casadei, R. Epis, L. Ferroni, I. Tocco, C. Gardin, E. Bressan, S. Sivolella, V. Vindigni, P. Pinton, G. Mucci, Biomed Res. Int. 2012 (2012).
[3] L.E. Kokai, K. Marra, J.P. Rubin, Transl. Res. 163 (2014) 399.
[4] Y.G. Illouz, A. Sterodimas, Aesthetic Plast. Surg. 33 (2009) 706.
[5] M. Cherubino, K.G. Marra, Regen. Med. (2009).
[6] A. Arkudas, J.P. Beier, K. Heidner, J. Tjiawi, E. Polykandriotis, S. Srour, M. Sturzl, R.E. Horch, U. Kneser, Tissue Eng. 13 (2007) 1549.
[7] M. Levy, N. Luciani, D. Alloyeau, D. Elgrabli, V. Deveaux, C. Pechoux, S. Chat, G. Wang, N. Vats, F. Gendron, Biomaterials 32 (2011) 3988.
[8] J.C. Ra, I.S. Shin, S.H. Kim, S.K. Kang, B.C. Kang, H.Y. Lee, Y.J. Kim, J.Y. Jo, E.J. Yoon, H.J. Choi, Stem Cells Dev. 20 (2011) 1297.
[9] S. Ramakrishna, J. Mayer, E. Wintermantel, K.W. Leong, Compos. Sci. Technol. 61 (2001) 1189.
[10] F. Pati, D.-H. Ha, J. Jang, H.H. Han, J.-W. Rhie, D.-W. Cho, Biomaterials 62 (2015) 164.
[11] K. Carrillo, G. Tamayo, A. Donohue, T. Kobayashi, R. Acuna, J. Tissue Sci. Eng. 6 (2015) 2.
[12] S. Kim, B.H. Shin, C. Yang, S. Jeong, J.H. Shim, M.H. Park, Y.B. Choy, C.Y. Heo, K. Lee, Polymers 10 (2018) 772.
[13] W.S. Kim, D.J. Mooney, P.R. Arany, K. Lee, N. Huebsch, J. Kim, Tissue Eng. A 18 (2012) 737.
[14] H. Tan, C.M. Ramirez, N. Miljkovic, H. Li, J.P. Rubin, K.G.J.B. Marra, Biomaterials 30 (2009) 6844.
[15] H.-W. Lee, S.J.C.-bi. Pyo, Chem. Biol. Interact. 298 (2019) 24.
[16] C. Patrick Jr, P. Chauvin, J. Hobley, G.P.J.T.e. Reece, Tissue Eng. 5 (1999) 139.
[17] S. Liu, H. Zhang, X. Zhang, W. Lu, X. Huang, H. Xie, J. Zhou, W. Wang, Y. Zhang, Y. Liu, Tissue Eng. A 17 (2011) 725.
[18] M.L. Moya, M.-H. Cheng, J.-J. Huang, M.E. Francis-Sedlak, S.-w. Kao, E.C. Opara, E.M.J.B. Brey, Biomaterials 31 (2010) 2816.
[19] J.S. Choi, H.-J. Yang, B.S. Kim, J.D. Kim, J.Y. Kim, B. Yoo, K. Park, H.Y. Lee, Y.W. Cho, J. Control Release 139 (2009) 2.
[20] Y. Itoi, M. Takatori, H. Hyakusoku, H.J.Jop. Mizuno, J. Plast. Reconstr. Aesthet. Surg. 63 (2010) 858.
[21] J.S. Kim, J.S. Choi, Y.W. Cho, Appl. Mater. Interfaces 9 (2017) 8581.
[22] L. Shukla, Y. Yuan, R. Shayan, D.W. Greening, T. Karnezis, Front. Pharmacol. 11 (2020) 158.
[23] H. Gloeckner, T. Jonuleit, H.-D. Lemke, J. Immunol. Methods 252 (2001) 131.
[24] K. Yoshimura, H. Suga, H. Eto, Regen. Med. (2009).
[25] K. Yoshimura, H. Eto, H. Kato, K. Doi, N.J.R.m. Aoi, Am. J. Clin. Pathol. 6 (2011) 33.
[26] A.R. Massensini, H. Ghuman, L.T. Saldin, C.J. Medberry, T.J. Keane, F.J. Nicholls, S. S. Velankar, S.F. Badylak, M. Modo, Acta Biomater. 27 (2015) 116.
[27] H. Wen, W. Xiao, S. Biswas, Z.-Q. Cong, X.-M. Liu, K.S. Lam, Y.-H. Liao, W. Deng, ACS Appl. Mater. Interfaces. 11 (2019) 5821.
[28] C.Y. Chen, C.J. Ke, K.C. Yen, H.C. Hsieh, J.S. Sun, F.H. Lin, Theranostics 5 (Mar (6)) (2015) 643.
[29] L. Hoareau, K. Bencharif, A.-C. Girard, L. Gence, P. Delarue, O. Hulard, F. Festy, R. Roche, J. Plast. Reconstr. Aesthet. Surg. 66 (2013) 712.
[30] R. Rajah, L. Katz, S. Nunn, P. Solberg, T. Beers, P. Cohen, Prog. Growth Factor Res. 6 (1995) 273.
[31] M.F. Gude, J. Frystyk, A. Flyvbjerg, J.M. Bruun, B. Richelsen, S.B.J.G.H. Pedersen, Growth Horm. IGF Res. 22 (2012) 200.
[32] S. Rajaram, D.J. Baylink, S. Mohan, Endocr. Rev. 18 (1997) 801.
[33] P.C. Heinrich, I. Behrmann, S. Haan, H.M. Hermanns, G. Müller-Newen, F. Schaper, Biochem J. 374 (2003) 1.
[34] T. Hirano, T. Taga, T. Matsuda, M. Hibi, S. Suematsu, B. Tang, M. Murakami, T. Kishimoto, J. Cell Cloning 8 (1990) 155.
[35] J.-P. Bastard, C. Jardel, J. Delattre, B. Hainque, E. Bruckert, F. Oberlin, Circulation 99 (1999) 2219c–2222.
[36] S. Liu, H. Zhang, X. Zhang, W. Lu, X. Huang, H. Xie, J. Zhou, W. Wang, Y. Zhang, Y. Liu, Z. Deng, Y. Jin, Tissue Eng. A. 17 (2011) 725.
[37] R. Armstrong, T. Harrower, C. Hurelbrink, M. McLaughin, E. Ratcliffe, P. Tyers, A. Richards, S. Dunnett, A.E. Rosser, R.J.N. Barker, Neuroscience 106 (2001) 201.
[38] P. Hogan, L. Duplock, M. Green, S. Smith, K.L. Gall, I.H. Frazer, M.F. O'Brien, C. Surgery, J. Thorac. 112 (1996) 1260.
[39] H. Eto, H. Kato, H. Suga, N. Aoi, K. Doi, S. Kuno, K. Yoshimura, Plast. Reconstr. Surg. 129 (2012) 1081.
[40] C.A. Carpaneda, M.T. Ribeiro, Aesth. Plast. Surg. 17 (1993) 43.
[41] S. Urs, C. Smith, B. Campbell, A.M. Saxton, J. Taylor, B. Zhang, J. Snoddy, B. Jones Voy, N. Moustaid-Moussa, J. Nutr. 134 (2004) 762.
[42] A.L. Ghaben, P.E. Scherer, Nat. Rev. Mol. Cell Biol. 20 (2019) 242.
[43] L. Makowski, K.C. Brittingham, J.M. Reynolds, J. Suttles, G.S. Hotamisligil, J. Biol. Chem. 280 (2005) 12888.
[44] M. Otero, R. Lago, F. Lago, F.F. Casanueva, C. Dieguez, J.J. Gómez-Reino, O. Gualillo, FEBS Lett. 579 (2) (2005) 295.